IET Optoelectronics

Special Issue on Optical-Wireless Communications

IET Journals
The Institution of Engineering and Technology

Performance evaluation of decode-and-forward dual-hop asymmetric radio frequency-free space optical communication system

ISSN 1751-8768
Received on 14th October 2014
Revised on 18th April 2015
Accepted on 5th May 2015
doi: 10.1049/iet-opt.2014.0118
www.ietdl.org

Sanya Anees[1], *Manav R. Bhatnagar*[2] ✉

[1]*Bharti School of Telecommunication Technology and Management, Indian Institute of Technology – Delhi, Hauz Khas, New Delhi 110016, India*
[2]*Department of Electrical Engineering, Indian Institute of Technology – Delhi, Hauz Khas, New Delhi 110016, India*
✉ *E-mail: manav@ee.iitd.ac.in*

Abstract: In this study, the error performance and the capacity analysis is performed for the decode-and-forward based dual-hop asymmetric radio frequency-free space optical communication (RF-FSO) system. The RF link is characterised by Nakagami-*m* fading and the FSO link is characterised by path loss, Gamma–Gamma distributed turbulence and pointing error. For this mixed RF-FSO cooperative system, novel closed-form mathematical expressions are derived for cumulative distribution function, probability density function and moment generating function of the equivalent signal-to-noise ratio in terms of Meijer-G function. Using these channel statistics, new finite power series based analytical expressions are obtained for the outage probability, the average bit error rate for various binary and *M*-ary modulation techniques and the average channel capacity of the considered system in terms of Meijer-G function. As a special case, the analytical framework can also be obtained for channel statistics and performance metrics of dual-hop mixed Rayleigh–Gamma–Gamma system. Simulation results validate the proposed mathematical analysis. The effects of fading, turbulence and pointing error are studied on the outage probability, average bit error rate and channel capacity of the asymmetric RF-FSO system.

1 Introduction

Free space optical (FSO) communication systems have various advantages like they require less power, cheap installation and operational cost with easy deployment, license-free spectrum, immunity to interference and large bandwidth capacity (10 Gbps); making them appealing for various applications in terrestrial and satellite communication [1, 2], for example, last mile access, backhauling services, data recovery, high definition transmission etc. However, the performance of the FSO systems is highly dependent on the atmospheric conditions, path loss and the pointing errors [1, 2]. The misalignment between the transmitter and the receiver of the system is caused because of the vibrations in the transmitted laser beams of tall buildings (resulting from wind, earthquakes, thermal expansion etc.) leading to pointing errors.

To minimise the effect of turbulence and pointing errors various solutions have been proposed such as Radio on FSO, in which radio frequency (RF) signals are transmitted through FSO links [3]; hyrbid RF/FSO, where the parallel RF link is used as a backup for FSO links [4], multiple-input multiple-output techniques [5] and cooperative communication [6–11]. Using the concepts of relaying technology in the FSO systems has many benefits – (i) increased coverage area from few kilometres to several kilometres [6] (ii) improved performance [9] (iii) enhanced capacity [11, 12]. One of the advantages of FSO systems is that they can be used for 'last mile access' as there exists a connectivity gap between the backbone network and the last- mile access network. Thus, the main back bone could be considered as the RF network and the high-speed FSO link can be used for connection to end users. Thus it would be beneficial to study the performance of mixed radio frequency-free space optical communication (RF-FSO) cooperative systems. In [6], the outage probability is derived for FSO cooperative systems using amplify-and-forward (AF) and decode-and-forward (DF) relays, where the channel is characterised by both path-loss as well as the Log-normal fading. For the first time dual hop mixed RF/FSO system was studied using an AF based relay from an outage probability point of view in [7], where the RF link was modelled by Rayleigh distribution and the FSO link was Gamma–Gamma distributed. A detailed study on an AF based dual-hop mixed RF-FSO cooperative communication system has been recently performed in [11]. In this set-up, a relay, with hybrid RF and optical capabilities, receives signals from the Nakagami-*m* fading RF link and forwards the received signals over the Gamma–Gamma fading FSO link, by using the subcarrier intensity modulation (SIM) scheme [13]. The effects of fading and pointing error are observed on the outage probability, BER and the average channel capacity of the considered system. As a special case, similar analysis was also performed for dual hop RF-FSO system where the RF link was Rayleigh distributed. In [14], a heterogeneous dual hop RF-FSO system is deployed and the end-to-end outage performance is investigated. The RF and FSO links are Rayleigh distributed and M-distributed, respectively, and the relay node use AF relaying protocol. In [15], ergodic capacity is analysed for AF based dual-hop FSO communication system by approximating the probability density function (PDF) of instantaneous SNR by $\alpha-\nu$ distribution. A multiuser DF based dual-hop cooperative system over mixed RF/FSO links is studied in [16]. The system comprises of multiple single-antenna sources, a DF relay and one destination equipped with a single photo-detector. Using the derived outage probability and BER analytical expressions the impact of pointing errors on the FSO link and the V-BLAST ordering effectiveness at the relay are investigated.

In this work, the analytical performance analysis of a dual-hop 'asymmetric' RF-FSO communication system is performed where the relay uses DF relaying protocol. The relay uses the SIM technique to transmit the optical signal and the destination uses direct detection technique. In the considered system, the RF link experiences Nakagami-*m* fading and the FSO link experiences Gamma–Gamma turbulence, path loss and pointing errors. Our

main contributions are: (i) New closed-form mathematical expressions are derived for statistical characteristics such as the cumulative distribution function (CDF), PDF and the moment generating function (MGF) of the asymmetric RF-FSO system in terms of Meijer-*G* function, when the FSO link is characterised by the atmospheric turbulence. (ii) Novel closed-form mathematical expressions are derived for CDF, PDF and MGF of the asymmetric RF-FSO system in terms of Meijer-G function, under the effect of turbulence, path loss and pointing error in the FSO link. (iii) Using (i), finite power series based novel analytical expression are obtained for the outage probability, the BER for various binary and *M*-ary modulation techniques and the ergodic channel capacity of the considered system in terms of Meijer-G function, where the FSO channel is characterised by the atmospheric turbulence only. (iv) Using (ii), finite power series based novel analytical expressions are obtained for the outage probability, the BER for various binary and *M*-ary modulation techniques and the ergodic channel capacity of the considered system in terms of Meijer-G function, where the FSO channel is characterised by the atmospheric turbulence, path loss and the pointing error. (v) As a special case, channel statistics and performance metrics are evaluated for DF based mixed Rayleigh–Gamma–Gamma cooperative system. (vi) With the help of (iii) and (iv), the effect of fading, turbulence and pointing error is analysed on outage probability, BER performance and average channel capacity of the DF based dual hop asymmetric RF-FSO communication system.

2 System model and statistical characteristics of RF and FSO links

Consider an asymmetric dual hop cooperative communication system; in this system, a source (S) communicates with a destination (D) via a relay node (R), as shown in Fig. 1. A scenario of mixed wireless communication is assumed, that is, the S-R link is Nakagami-*m* distributed RF link and R-D link is a FSO link characterised by path loss, Gamma–Gamma distributed turbulence and pointing errors. In Fig. 1, $\gamma_{s,r}$ and $\gamma_{r,d}$ are the instantaneous signal-to-noise ratios (SNRs) of the S-R and the R-D links, respectively, $\sigma_{s,r}^2$ and $\sigma_{r,d}^2$ are the AWGN variances of the S-R and the R-D links, respectively, $m \geq 1/2$ is the Nakagami fading parameter; a and b are the atmospheric turbulence parameters which depend upon the FSO link length, L, operating wavelength, λ and the refractive-index structure parameter, C_n^2, as $a = \left[\exp\left(0.49\sigma_l^2/(1+1.11\sigma_l^{12/5})^{7/6}\right)-1\right]^{-1}$ and $b = \left[\exp\left(0.51\sigma_l^2/(1+0.69\sigma_l^{12/5})^{5/6}\right)-1\right]^{-1}$, where the Rytov variance $\sigma_l^2 = 1.23C_n^2k^{7/6}L^{11/6}$, in which wave number $k = 2\pi/\lambda$ [12, 13]. The relay contains hybrid capabilities; it decodes the data transmitted by S and transmits the newly encoded data over the FSO link to D, by using SIM scheme. In the SIM process, an RF subcarrier signal is first modulated with the message and then is used to modulate the intensity of the optical source. Thus the subcarrier can be modulated by any of the standard RF modulation techniques, such as *M*-ary amplitude shift keying (*M*-ASK), *M*-ary frequency shift keying (*M*-FSK), *M*-ary phase shift keying (*M*-PSK), *M*-ary quadrature amplitude modulation (*M*-QAM) etc. At the destination, the incoming optical radiation is converted into an electrical signal using direct detection technique and then de-modulated by the RF demodulator to recover the transmitted symbol [13].

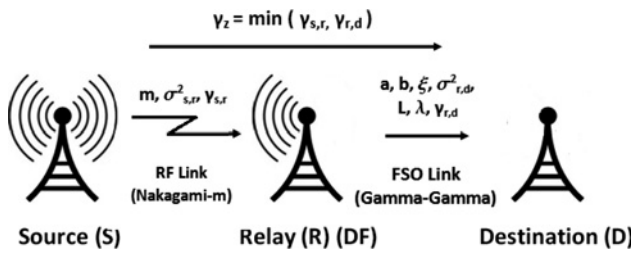

Fig. 1 *System Model of DF based dual-hop asymmetric RF-FSO system*

The signal received by *R*, through the RF link, can be expressed as

$$y_{s,r} = h_{s,r}x + e_{s,r} \tag{1}$$

where x, with average energy $E_{s,r}$, denotes the signal transmitted by S, e_{sr} represents the complex-valued additive white Gaussian noise (AWGN) with zero-mean and $\sigma_{s,r}^2$ variance and $h_{s,r}$ denotes the Nakagami-*m* distributed channel gain of the S-R link. From (1), $\gamma_{s,r} = E_{s,r}|h_{s,r}|^2/\sigma_{s,r}^2 = |h_{s,r}|^2\bar{\gamma}_{s,r}$, where $\bar{\gamma}_{s,r} = E_{s,r}/\sigma_{s,r}^2$ denotes the average SNR of the S-R link. The PDF of $\gamma_{s,r}$ is given by

$$f_{\gamma_{s,r}}(\gamma) = \frac{m^m\gamma^{m-1}}{\Gamma(m)\bar{\gamma}_{s,r}^m}\exp\left(-\frac{m\gamma}{\bar{\gamma}_{s,r}}\right) \tag{2}$$

where $\Gamma(\cdot)$ is the Gamma function.

The signal received by D from DF based R, over the FSO link after optical-to-electrical conversion, can be written as

$$y_{r,d} = \eta_{r,d}I_{r,d}\hat{x} + e_{r,d} \tag{3}$$

where $\hat{x}$, with unit average power, is the estimate of x in R, $\eta_{r,d}$ is the optical-to-electrical conversion coefficient, $e_{r,d}$ denotes the zero-mean AWGN noise with variance, $\sigma_{r,d}^2$ and $I_{r,d}$ with $E\{I_{r,d}\} = 1$, where $E\{\cdot\}$ stands for expectation, represents the real-valued Gamma–Gamma distributed intensity of the R-D link. In the FSO link, the total degradation $I_{r,d}$ is product of path loss I_l, pointing error I_p and atmospheric turbulence I_a, that is, $I_{r,d} = I_lI_pI_a$ where I_p and I_a are random distributions and I_l is deterministic.

DF transmission involves examination of symbol-by-symbol decoding at the relay. The maximum transmission rate for DF based dual hop system is minimum of two random variables – (i) maximum rate at which R can reliably decode the source message and (ii) maximum rate at which D can reliably decode the source message given repeated transmissions between S-D. [17]. Thus the instantaneous received SNR at D, γ_z, for a DF based dual hop cooperative system is written as [16, 17]

$$\gamma_z = \min(\gamma_{s,r}, \gamma_{r,d}) \tag{4}$$

where by using (3), $\gamma_{r,d} = \eta_{r,d}^2I_{r,d}^2/\sigma_{r,d}^2$ and the electrical SNR is given by, $\bar{\gamma}_{r,d} = \eta_{r,d}^2E[I_{r,d}]^2/\sigma_{r,d}^2 = \eta_{r,d}^2/\sigma_{r,d}^2$. The average SNR, $\gamma_{a_{r,d}}$, of the R-D link can be easily computed as $\gamma_{a_{r,d}} = ((a+1)(b+1)/ab)\gamma_{r,d}$ [18].

2.1 Channel model under atmospheric turbulence

If the FSO link is assumed to undergo Gamma–Gamma turbulence only, then the PDF of $\gamma_{r,d}$ is given by

$$f_{\gamma_{r,d}}(\gamma) = \frac{(ab)^{(a+b)/2}\gamma^{((a+b)/4)-1}}{\Gamma(a)\Gamma(b)\bar{\gamma}_{r,d}^{(a+b)/4}}K_{a-b}\left(2\sqrt{ab\sqrt{\frac{\gamma}{\bar{\gamma}_{r,d}}}}\right) \tag{5}$$

Using (5) and $F_{\gamma_{r,d}}(\gamma) = \int_0^\gamma f_{\gamma_{r,d}}(\gamma)\,\mathrm{d}\gamma$, the CDF of $\gamma_{r,d}$ can be derived as

$$F_{\gamma_{r,d}}(\gamma) = \frac{(ab)^{z_1/2}\left(\gamma/\sqrt{\bar{\gamma}_{r,d}}\right)^{z_1/4}}{\Gamma(a)\Gamma(b)}G_{1,3}^{2,1}\left(ab\sqrt{\frac{\gamma}{\bar{\gamma}_{r,d}}}\middle|\begin{matrix}1-\frac{z_1}{2}\\ \frac{z_2}{2}, -\frac{z_2}{2}, \frac{-z_1}{2}\end{matrix}\right) \tag{6}$$

where $z_1 = a+b$, $z_2 = a-b$ and $G(\cdot)$ is the Meijer-*G* function [19].

2.2 Channel model under the combined effect of path loss, atmospheric turbulence and pointing error

Similar to the PDF of instantaneous SNR given in [20], the instantaneous received SNR $\gamma_{r,d}$ in case of direct detection, will have the following PDF

$$f_{\gamma_{rd}}(\gamma) = \frac{\xi^2}{2\gamma\Gamma(a)\Gamma(b)} G_{1,3}^{3,0}\left(pab\sqrt{\frac{\gamma}{\bar{\gamma}_{r,d}}} \middle| \begin{matrix} \xi^2+1 \\ \xi^2, a, b \end{matrix} \right) \tag{7}$$

where $\gamma = \bar{\gamma}_{r,d}/h_l A_0 p$, $p = \xi^2/(\xi^2+1)$, $\mathcal{A}_0 = [\mathrm{erf}(\nu_{p,q})]^2$, $\nu = \sqrt{\pi/2}R/w_b$, $\xi = w_e/(2\sigma_s)$, erf(·) denotes the error function, R is the radius of the receiver aperture, w_b is the normalised beamwaist, w_e is the equivalent beamwaist and σ_s is the pointing error displacement standard deviation at the receiver.

The CDF of $\gamma_{r,d}$ in this scenario can be derived using (7) and [19, Eq (8.2.2.19), Eq (1.16.2.1)] as

$$F_{\gamma_{r,d}}(\gamma) = \frac{2^{z_1-2}\xi^2}{2\pi\Gamma(a)\Gamma(b)} G_{3,7}^{6,1} \left(\frac{(pab)^2\gamma}{16\bar{\gamma}_{r,d}} \middle| \begin{matrix} 1, \frac{\xi^2+1}{2}, \frac{\xi^2+2}{2} \\ \frac{\xi^2}{2}, \frac{\xi^2+1}{2}, \frac{a}{2}, \frac{a+1}{2}, \frac{b}{2}, \frac{b+1}{2}, 0 \end{matrix} \right) \tag{8}$$

3 Statistical characteristics of dual hop DF based mixed RF-FSO system

The mathematical expressions of CDF, PDF and MGF of the DF based dual-hop asymmetric RF-FSO systems are derived for the following two scenarios, considering only turbulence in the FSO link in the first scenario and combined effect of turbulence, path loss and pointing error in the FSO link in the second scenario.

3.1 Under atmospheric turbulence

When the RF link experiences Nakagami-m fading and the FSO link experiences Gamma–Gamma distributed turbulence, the statistical characteristics are obtained as follows.

3.1.1 Cumulative distribution function: Using (4), the CDF of the equivalent SNR (γ_z) for the considered RF-FSO system is given by

$$F_{\gamma_Z}(\gamma) = F_{\gamma_{s,r}}(\gamma) + F_{\gamma_{r,d}}(\gamma) - F_{\gamma_{s,r}}(\gamma)F_{\gamma_{r,d}}(\gamma) \tag{9}$$

where $F_{\gamma_{s,r}}$ is the CDF of the instantaneous SNR of the S-R link.

Using the relation

$$F_X(x) = \int_{-\infty}^{x} f_X(t)\,\mathrm{d}t \tag{10}$$

(2) and (6), in (9), the CDF of γ_z can be written as

$$F_{\gamma_z}(\gamma) = 1 - \left(1 - \mathcal{K}_1\gamma\left(m, \frac{m\gamma}{\bar{\gamma}_{s,r}}\right)\right) \times \left(1 - \mathcal{K}_2\gamma^{z_1/4} G_{1,3}^{2,1}\left(\mathcal{W}_1\sqrt{\gamma} \middle| \begin{matrix} 1-\frac{z_1}{2} \\ \frac{z_2}{2}, -\frac{z_2}{2}, -\frac{z_1}{2} \end{matrix} \right)\right) \tag{11}$$

where $\gamma(s,x) = \int_0^x t^{s-1}\mathrm{e}^{-t}\,\mathrm{d}t$ represents the lower incomplete Gamma function, $\mathcal{K}_1 = 1/\Gamma(m)$, $\mathcal{K}_2 = (1/\Gamma(a)\Gamma(b))\left(ab/\sqrt{\bar{\gamma}_{r,d}}\right)$ and $\mathcal{W}_1 = ab/\sqrt{\bar{\gamma}_{r,d}}$.

3.1.2 Probability density function: The PDF of the equivalent SNR for the DF based dual hop system is given by using (4) as

$$f_{\gamma_Z}(\gamma) = f_{\gamma_{s,r}}(\gamma) + f_{\gamma_{r,d}}(\gamma) - f_{\gamma_{s,r}}(\gamma)F_{\gamma_{r,d}}(\gamma) - F_{\gamma_{s,r}}(\gamma)f_{\gamma_{r,d}}(\gamma) \tag{12}$$

Using (2), (5), (6) and (10) in (12), the PDF can be obtained as

$$f_{\gamma_z}(\gamma) = \left(\mathcal{K}_1\left(\frac{m}{\bar{\gamma}_{s,r}}\right)^m \gamma^{m-1}\exp\left(\frac{-m\gamma}{\bar{\gamma}_{s,r}}\right)\right) \times \left(1 - \mathcal{K}_2\gamma^{z_1/4} G_{1,3}^{2,1}\left(\mathcal{W}_1\sqrt{\gamma} \middle| \begin{matrix} 1-\frac{z_1}{2} \\ \frac{z_2}{2}, -\frac{z_2}{2}, -\frac{z_1}{2} \end{matrix} \right)\right) + \left(1 - \mathcal{K}_1\gamma\left(m, \frac{m\gamma}{\bar{\gamma}_{s,r}}\right)\right)\left(\mathcal{K}_2\gamma^{(z_1/4)-1}K_{a-b}\left(2\sqrt{\mathcal{W}_1\sqrt{\gamma}}\right)\right) \tag{13}$$

3.1.3 Moment generating function: The MGF generally defined in terms of the PDF is given by [21, Eq. (5–96)]

$$\mathcal{M}_\gamma(s) \triangleq \int_{-\infty}^{\infty} \mathrm{e}^{-s\gamma} f_{\gamma_z}(\gamma)\,\mathrm{d}\gamma \tag{14}$$

Substituting (13) in (14) and using the series expansion of the lower incomplete Gamma function

$$\gamma(m,x) = (m-1)!\left(1 - \mathrm{e}^{-x}\sum_{k=0}^{m-1}\frac{x^k}{k!}\right) \tag{15}$$

[19, Eq. (8.4.23.1), Eq. (8.2.2.19)], [22, Eq. (5.6.3.1)], the MGF for the considered system can be derived as

$$\mathcal{M}_{\gamma_z}(s) = \left(\frac{m}{m+s\bar{\gamma}_{s,r}}\right)^m - \frac{\mathcal{K}_1\mathcal{K}_2}{4\pi}\left(\frac{m}{\bar{\gamma}_{s,r}}\right)^m \left(s+\frac{m}{\bar{\gamma}_{s,r}}\right)^{-(z_1/4)-m} \times G_{3,6}^{4,3}\left(\mathcal{W}_3 \middle| \begin{matrix} 1-\frac{z_1}{4}-m, \mathcal{P}_1 \\ \mathcal{P}_2, \frac{-z_1}{4}, \frac{-z_1+2}{4} \end{matrix} \right) + \sum_{k=0}^{m-1}\mathcal{K}_3 \times \left(s+\frac{m}{\bar{\gamma}_{s,r}}\right)^{-(z_1/4)-k} G_{1,4}^{4,1}\left(\mathcal{W}_3 \middle| \begin{matrix} 1-\frac{z_1}{4}-k \\ \mathcal{P}_2 \end{matrix} \right) \tag{16}$$

where $\mathcal{W}_2 = (ab)^2/16\bar{\gamma}_{r,d}$, $\mathcal{W}_3 = \mathcal{W}_2\bar{\gamma}_{s,r}/(m+s\bar{\gamma}_{s,r})$, $\mathcal{P}_1 = (-z_1+2)/4, (-z_1+4)/4$, $\mathcal{P}_2 = z_2/4, (z_2+2)/4, -z_2/4, (-z_2+2)/4$ and $\mathcal{K}_3 = (\mathcal{K}_2/4\pi k!)\left(m/\bar{\gamma}_{s,r}\right)^k$.

3.2 Under the combined effect of path loss, atmospheric turbulence and pointing error

When the RF link is characterised by the Nakagami-m fading and the FSO link is characterised by the path loss, Gamma–Gamma distributed turbulence and pointing error, the statistical characteristics are obtained as follows.

3.2.1 Cumulative distribution function: Using (2), (8) and (10) in (9), we obtain

$$F_{\gamma_z}(\gamma) = 1 - \left(1 - \mathcal{K}_1\gamma\left(m, \frac{m\gamma}{\bar{\gamma}_{s,r}}\right)\right) \times \left(1 - \mathcal{K}_4 G_{3,7}^{6,1}\left(\mathcal{W}_4\gamma \middle| \begin{matrix} 1, \mathcal{P}_3 \\ \mathcal{P}_4, 0 \end{matrix} \right)\right) \tag{17}$$

where $\mathcal{K}_4 = 2^{z_1-2}\xi^2/(2\pi\Gamma(a)\Gamma(b))$, $\mathcal{W}_4 = (pab)^2/(16\gamma_{r,d})$, $\mathcal{P}_3 = (\xi^2+1)/2, (\xi^2+2)/2$ and $\mathcal{P}_4 = \xi^2/2, (\xi^2+1)/2, a/2, (a+1)/2, b/2, (b+1)/2$.

3.2.2 Probability density function: Substituting (2), (7), (8) and (10) in (12), the PDF can be obtained as

$$f_{\gamma_z}(\gamma) = \left(\mathcal{K}_1\left(\frac{m}{\bar{\gamma}_{s,r}}\right)^m \gamma^{m-1}\exp\left(\frac{-m\gamma}{\bar{\gamma}_{s,r}}\right)\right) \times \left(1-\mathcal{K}_4 G_{3,7}^{6,1}\left(\mathcal{W}_4\gamma\middle|\begin{matrix}1, \mathcal{P}_3\\ \mathcal{P}_4, 0\end{matrix}\right)\right) + \mathcal{K}_4\gamma^{-1}\left(1-\mathcal{K}_1\gamma\left(m, \frac{m\gamma}{\bar{\gamma}_{s,r}}\right)\right) G_{2,6}^{6,0}\left(\mathcal{W}_4\gamma\middle|\begin{matrix}\mathcal{P}_3\\ \mathcal{P}_4\end{matrix}\right) \quad (18)$$

3.2.3 Moment generating function: Substituting (18) in (14) and then using [19, Eq. (8.2.19)] and [22, Eq. (5.6.3.1)], the MGF for the considered system with significant pointing errors is given by

$$\mathcal{M}_{\gamma_z}(s) = \left(\frac{m}{m+s\bar{\gamma}_{s,r}}\right)^m - \mathcal{K}_1\mathcal{K}_4\left(\frac{m}{m+s\bar{\gamma}_{s,r}}\right)^m \times G_{4,7}^{6,2}\left(\mathcal{W}_5\middle|\begin{matrix}1-m, 1, \mathcal{P}_3\\ \mathcal{P}_4, 0\end{matrix}\right) + \sum_{k=0}^{m-1}\frac{\mathcal{K}_4}{k!} \times \left(\frac{m}{m+s\bar{\gamma}_{s,r}}\right)^k G_{3,6}^{6,1}\left(\mathcal{W}_5\middle|\begin{matrix}1-k, \mathcal{P}_3\\ \mathcal{P}_4\end{matrix}\right) \quad (19)$$

where $\mathcal{W}_5 = \mathcal{W}_4\bar{\gamma}_{s,r}/(m+s\bar{\gamma}_{s,r})$.

4 Performance of the dual-hop asymmetric RF/FSO cooperative system

In this section, the finite power series mathematical expressions are derived for outage probability, BER and average capacity of the DF based dual-hop mixed RF-FSO systems for following cases.

4.1 Under atmospheric turbulence

4.1.1 Outage probability: Outage probability is defined as the probability at which the equivalent SNR, γ_z, falls below a predetermined threshold value γ_{th}. The outage probability for the DF based dual hop RF-FSO cooperative system under no pointing error can be derived by using (11) as

$$P_{\text{out}}(\gamma_{\text{th}}) = 1 - \left(1-\mathcal{K}_1\gamma\left(m, \frac{m\gamma_{\text{th}}}{\bar{\gamma}_{s,r}}\right)\right) \times \left(1-\mathcal{K}_2\gamma_{th}^{z_1/4} G_{1,3}^{2,1}\left(\mathcal{W}_1\sqrt{\gamma_{\text{th}}}\middle|\begin{matrix}1-\frac{z_1}{2}\\ \frac{z_2}{2}, -\frac{z_2}{2}, -\frac{z_1}{2}\end{matrix}\right)\right) \quad (20)$$

4.1.2 Average bit error rate: In this section, the BER of the DF based mixed RF-FSO system is derived for various binary modulation techniques, M-QAM and M-PSK under no pointing errors.

(a) *Binary modulation techniques:* Using [23, Eq. (12)], the average BER for the considered cooperative system is expressed by

$$P_{e_b} = \frac{y^x}{2\Gamma(x)}\int_0^\infty \gamma^{x-1}\exp(-y\gamma)F_{\gamma_z}(\gamma)\,\mathrm{d}\gamma \quad (21)$$

Table 1 Parameters (x and y) for various binary modulation techniques [22]

Modulation techniques	x	y
coherent binary frequency shift keying (CBFSK)	0.5	0.5
coherent binary phase shift keying (CBPSK)	0.5	1
non-coherent binary frequency shift keying (NBFSK)	1	0.5
differential binary phase shift keying (DBPSK)	1	1

where x and y are the BER parameters describing various binary modulation techniques [23] given in Table 1. Substituting (11) in (21) and using [22, Eq. (5.6.3.1)], the mathematical expression for the BER for binary modulation techniques is given by

$$P_{e_b} = \frac{\mathcal{K}_1}{2\Gamma(x)} G_{2,2}^{1,2}\left(\frac{m}{y\bar{\gamma}_{s,r}}\middle|\begin{matrix}1-x, 1\\ m, 0\end{matrix}\right) + \sum_{k=0}^{m-1}\frac{y^x\mathcal{K}_3}{2\Gamma(x)}\left(y+\frac{m}{\bar{\gamma}_{s,r}}\right)^{(-z_1/4)-x-k} \times G_{3,6}^{4,3}\left(\frac{\mathcal{W}_2\bar{\gamma}_{s,r}}{m+y\bar{\gamma}_{s,r}}\middle|\begin{matrix}1-\frac{z_1}{4}-x-k, \mathcal{P}_1\\ \mathcal{P}_2, \frac{-z_1}{4}, \frac{-z_1+2}{4}\end{matrix}\right) \quad (22)$$

(b) *M-PSK*: The instantaneous BER of the M-PSK modulation technique can be written as [24]

$$P_e(\gamma) \simeq \frac{2}{\Psi_M}\sum_{j=1}^{T} Q\left(a_j\sqrt{2\gamma}\right) \quad (23)$$

where $Q(.)$ is the Q-function, $\Psi_M = \max(\log_2 M, 2)$, $T = \max(M/4, 1)$ and $a_j = \sin((2j-1)\pi/M)$. The average BER is expressed as

$$P_e = \int_0^\infty P_e(\gamma)f_{\gamma_Z}(\gamma)\,\mathrm{d}\gamma = -\int_0^\infty F_{\gamma_Z}(\gamma)\,\mathrm{d}P_e(\gamma) \quad (24)$$

Solving the integral in (24) by substituting (11) and (23) in it and then using [22, Eq. (5.6.3.1)], the BER for the mixed RF-FSO system employing M-PSK constellation is derived as

$$P_{e_p} \simeq \sum_{j=1}^{T}\frac{\mathcal{K}_1}{\sqrt{\pi}\Psi_M} G_{2,2}^{1,2}\left(\frac{m}{a_j^2\bar{\gamma}_{s,r}}\middle|\begin{matrix}\frac{1}{2}, 1\\ m, 0\end{matrix}\right) + \sum_{j=1}^{T}\sum_{k=0}^{m-1}\frac{a_j\mathcal{K}_3}{\sqrt{\pi}\Psi_M} \times \left(a_j^2+\frac{m}{\bar{\gamma}_{s,r}}\right)^{(-z_1/4)-k-(1/2)} \times G_{3,6}^{4,3}\left(\frac{\mathcal{W}_2\bar{\gamma}_{s,r}}{m+a_j^2\bar{\gamma}_{s,r}}\middle|\begin{matrix}\frac{1}{2}-\frac{z_1}{4}-k, \mathcal{P}_1\\ \mathcal{P}_2, \frac{-z_1}{4}, \frac{-z_1+2}{4}\end{matrix}\right) \quad (25)$$

(c) *M-QAM:* The instantaneous BER of the M-QAM modulation scheme can be written as [24]

$$P_e(\gamma) \simeq 4\Upsilon_M\sum_{j=1}^{\sqrt{M}/2} Q\left(b_j\sqrt{\gamma}\right) \quad (26)$$

where $\Upsilon_M = (1/\log_2 M)\left(1-(1/\sqrt{M})\right)$ and $b_j = (2j-1)\times\sqrt{3/(M-1)}$.

Substituting (11) and (26) in (24) and using [22, Eq. (5.6.3.1)], the BER for the asymmetric RF-FSO system employing M-QAM

constellation is obtained as

$$P_{e_q} \simeq \sum_{j=1}^{\sqrt{M}/2} \frac{2\mathcal{K}_1 \Upsilon_M}{\sqrt{\pi}} G_{2,2}^{1,2}\left(\frac{2m}{b_j^2 \bar{\gamma}_{s,r}}\middle|\begin{matrix}\frac{1}{2}, 1\\ m, 0\end{matrix}\right) + \sum_{j=1}^{\sqrt{M}/2}\sum_{k=0}^{m-1}\sqrt{\frac{2}{\pi}} b_j \mathcal{K}_3 \times \Upsilon_M\left(\frac{b_j^2}{2}+\frac{m}{\bar{\gamma}_{s,r}}\right)^{(-z_1/4)-k-(1/2)} \times G_{3,6}^{4,3}\left(\frac{2\mathcal{W}_2 \bar{\gamma}_{s,r}}{2m+b_j^2\bar{\gamma}_{s,r}}\middle|\begin{matrix}\frac{1}{2}-\frac{z_1}{4}-k, \mathcal{P}_1\\ \mathcal{P}_2, \frac{-z_1}{4}, \frac{-z_1+2}{4}\end{matrix}\right) \quad (27)$$

4.1.3 Average channel capacity: The average channel capacity can be expressed in terms of MGF as [25]

$$C_{\text{avg}} \simeq \frac{B}{\log 2}\sum_{n=1}^{N} v_n Ei(-s_n)\left[\frac{\delta}{\delta s} M_\gamma(s)\middle|_{s\to s_n}\right] \quad (28)$$

where B is the bandwidth, N is a positive integer

$$v_n = \frac{\pi^2 \sin\big(((2n-1)/2N)\pi\big)}{4N\cos^2\big((\pi/4)\cos\big(((2n-1)/2N)\pi\big)+(\pi/4)\big)},$$
$$s_n = \tan\left(\frac{\pi}{4}\cos\left(\frac{2n-1}{2N}\pi\right)+\frac{\pi}{4}\right)$$

and $Ei(x)$ is the exponential integral function. This approximation converges very fast requiring very less number of terms to obtain an exact match with the simulation result.

Substituting (13) and (14) in (28) and using [22, Eq. (5.6.3.1)], the capacity of the dual hop AF based mixed RF-FSO system is obtained as

$$C_{\text{avg}} \simeq \frac{B}{\log 2}\sum_{n=1}^{N} v_n Ei(-s_n)\Bigg[-\left(\frac{m}{m+s_n\bar{\gamma}_{s,r}}\right)^{m+1}\bar{\gamma}_{s,r} + \frac{\mathcal{K}_1\mathcal{K}_2}{4\pi}\left(\frac{m}{\bar{\gamma}_{s,r}}\right)^m\left(s+\frac{m}{\gamma_{s,r}}\right)^{(-z_1/4)-m-1} \times G_{3,6}^{4,3}\left(\mathcal{W}_3'\middle|\begin{matrix}\frac{-z_1}{4}-m, \mathcal{P}_1\\ \mathcal{P}_2, \frac{-z_1}{4}, \frac{-z_1+2}{4}\end{matrix}\right) - \sum_{k=0}^{m-1}\mathcal{K}_3\left(s_n+\frac{m}{\bar{\gamma}_{s,r}}\right)^{-(z_1/4)-k-1} G_{1,4}^{4,1}\left(\mathcal{W}_3'\middle|\begin{matrix}-\frac{z_1}{4}-k\\ \mathcal{P}_2\end{matrix}\right)\Bigg] \quad (29)$$

where $\mathcal{W}_3' = \mathcal{W}_2\bar{\gamma}_{s,r}/(m+s_n\bar{\gamma}_{s,r})$.

4.2 Under the combined effect of path loss, atmospheric turbulence and pointing error

4.2.1 Outage probability: The end-to-end outage probability for the DF based dual hop RF/FSO system under the influence of fading, turbulence and pointing errors can be obtained using (17) as

$$P_{\text{out}}(\gamma_{\text{th}}) = 1 - \left(1-\mathcal{K}_1\gamma\left(m, \frac{m\gamma_{\text{th}}}{\bar{\gamma}_{s,r}}\right)\right) \times \left(1-\mathcal{K}_4 G_{3,7}^{6,1}\left(\mathcal{W}_4\gamma_{\text{th}}\middle|\begin{matrix}1, \mathcal{P}_3\\ \mathcal{P}_4, 0\end{matrix}\right)\right) \quad (30)$$

4.2.2 Average bit error rate: In this section, the BER of the considered asymmetric system is derived for various modulation techniques considering significant pointing error.

(a) *Binary modulation techniques:* Substituting (17) in (21) and then using [22, Eq. (5.6.3.1)], the closed form mathematical expression for the BER is given by

$$P_e = \frac{\mathcal{K}_1}{2\Gamma(x)} G_{2,2}^{1,2}\left(\frac{m}{y\bar{\gamma}_{s,r}}\middle|\begin{matrix}1-x, 1\\ m, 0\end{matrix}\right) + \sum_{k=0}^{m-1}\frac{y^x\mathcal{K}_4}{2k!\Gamma(x)}\left(\frac{m}{\bar{\gamma}_{s,r}}\right)^k \times \left(y+\frac{m}{\bar{\gamma}_{s,r}}\right)^{-x-k} G_{4,7}^{6,2}\left(\frac{\mathcal{W}_4\bar{\gamma}_{s,r}}{m+y\bar{\gamma}_{s,r}}\middle|\begin{matrix}1-x-k, 1, \mathcal{P}_3\\ \mathcal{P}_4, 0\end{matrix}\right) \quad (31)$$

(b) *M-PSK:* Substituting (17) and (23) in (24) and then using [22, Eq. (5.6.3.1)], the BER for the considered RF-FSO system employing M-PSK constellation is given by

$$P_{e_p} \simeq \sum_{j=1}^{T}\frac{\mathcal{K}_1}{\sqrt{\pi}\Psi_M} G_{2,2}^{1,2}\left(\frac{m}{a_j^2\bar{\gamma}_{s,r}}\middle|\begin{matrix}\frac{1}{2}, 1\\ m, 0\end{matrix}\right) + \sum_{j=1}^{T}\sum_{k=0}^{m-1}\frac{a_j\mathcal{K}_4}{\sqrt{\pi}\Psi_M k!} \times \left(\frac{m}{\bar{\gamma}_{s,r}}\right)^k\left(a_j^2+\frac{m}{\bar{\gamma}_{s,r}}\right)^{(-1/2)-k} \times G_{4,7}^{6,2}\left(\frac{\mathcal{W}_4\bar{\gamma}_{s,r}}{m+a_j^2\bar{\gamma}_{s,r}}\middle|\begin{matrix}\frac{1}{2}-k, 1, \mathcal{P}_3\\ \mathcal{P}_4, 0\end{matrix}\right) \quad (32)$$

(c) *M-QAM:* Solving the integral in (24) by substituting (17) and (26) in it and using [22, Eq. (5.6.3.1)], the BER for the asymmetric RF-FSO system employing M-QAM constellation is obtained as

$$P_{e_q} \simeq \sum_{j=1}^{\sqrt{M}/2}\frac{2\mathcal{K}_1\Upsilon_M}{\sqrt{\pi}} G_{2,2}^{1,2}\left(\frac{2m}{b_j^2\bar{\gamma}_{s,r}}\middle|\begin{matrix}\frac{1}{2}, 1\\ m, 0\end{matrix}\right) + \sum_{j=1}^{\sqrt{M}/2}\sum_{k=0}^{m-1}\sqrt{\frac{2}{\pi}}\frac{b_j\mathcal{K}_4}{k!} \times \Upsilon_M\left(\frac{m}{\bar{\gamma}_{s,r}}\right)^k\left(\frac{b_j^2}{2}+\frac{m}{\bar{\gamma}_{s,r}}\right)^{-k-(1/2)} \times G_{4,7}^{6,2}\left(\frac{2\mathcal{W}_4\bar{\gamma}_{s,r}}{2m+b_j^2\bar{\gamma}_{s,r}}\middle|\begin{matrix}\frac{1}{2}-k, 1, \mathcal{P}_3\\ \mathcal{P}_4, 0\end{matrix}\right) \quad (33)$$

4.3 Average channel capacity

Substituting (14) and (18) in (28) and using [22, Eq. (5.6.3.1)], the capacity of the dual hop AF based mixed RF-FSO system for significant pointing errors is obtained as

$$C_{\text{avg}} \simeq \frac{B}{\log 2}\sum_{n=1}^{N} v_n Ei(-s_n)\Bigg[-\left(\frac{m}{m+s_n\bar{\gamma}_{s,r}}\right)^{m+1}\bar{\gamma}_{s,r} + \mathcal{K}_1\mathcal{K}_4\left(\frac{m}{\bar{\gamma}_{s,r}}\right)^m\left(\frac{m+s_n\bar{\gamma}_{s,r}}{\bar{\gamma}_{s,r}}\right)^{-m-1} G_{4,7}^{6,2}\left(\mathcal{W}_5'\middle|\begin{matrix}-m, 1, \mathcal{P}_3\\ \mathcal{P}_4, 0\end{matrix}\right) - \sum_{k=0}^{m-1}\frac{\mathcal{K}_4}{k!}\left(\frac{m}{\bar{\gamma}_{s,r}}\right)^k\left(\frac{m+s_n\bar{\gamma}_{s,r}}{\bar{\gamma}_{s,r}}\right)^{-k-1} G_{3,6}^{6,1}\left(\mathcal{W}_5'\middle|\begin{matrix}-k, \mathcal{P}_3\\ \mathcal{P}_4\end{matrix}\right)\Bigg] \quad (34)$$

where $\mathcal{W}_5' = \mathcal{W}_4\bar{\gamma}_{s,r}/(m+s_n\bar{\gamma}_{s,r})$.

As a special case, mathematical expressions can be obtained for all the channel statistics and performance metrics of dual hop DF based mixed RF-FSO system where the RF link is modelled by Rayleigh fading and the FSO link is modelled by Gamma–Gamma turbulence, by substituting Nakagami-m parameter as $m=1$ in (11), (13), (16)–(20), (22), (25), (27), (29)–(34).

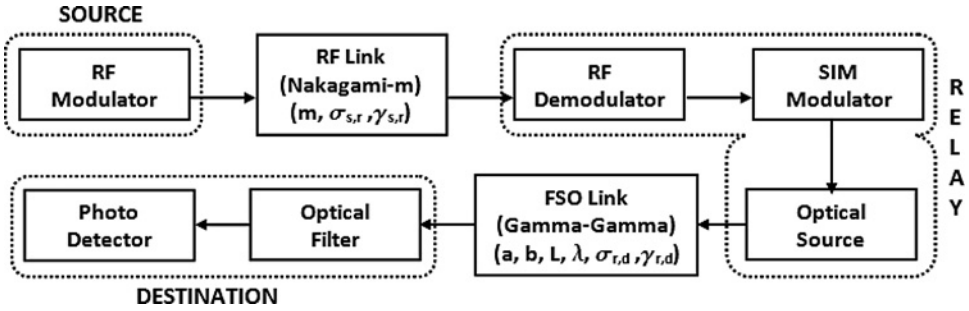

Fig. 2 *Simulation setup of DF based dual-hop asymmetric RF-FSO system*

Table 2 Simulation parameters

Parameter	Value
link length	2000 m
wavelength	1550 nm
transmit optical power	1 W
responsivity	0.9

Table 3 FSO link fading parameters [9, 13]

Rytov variance	Turbulence parameters	Scintillation index
1.6	$a = 4.0$, $b = 1.9$	0.9
3.5	$a = 4.2$, $b = 1.4$	1.14

5 Numerical results

In this section, the numerical results for the outage probability, the average BER and the average capacity are discussed for the considered DF based dual hop asymmetric RF-FSO communication system. The RF link experiences Nakagami-*m* fading, characterising weak to strong fading and the FSO link experiences Gamma–Gamma turbulence, characterising weak to strong turbulence along with path loss and pointing error. Fig. 2 shows the simulation setup used where source consists of RF modulator, relay consists of RF demodulator, SIM modulator where pre-modulated RF subcarrier modulates the intensity of the optical source and destination consists of optical filter and photodetector which converts the optical signal to electrical signal. The FSO link simulation parameters and fading parameters are given in Tables 2 and 3, respectively. We know that almost all the commercially available FSO systems operate in the wavelength range of $0.60\ \mu m < \lambda < 1.55\ \mu m$ and that the attenuation inversely depends on the wavelength [26]. Thus in our paper, 1.55 μm wavelength is assumed because it undergoes least smoke and fog attenuation, making it favourable for varied atmospheric conditions. It is assumed that the average SNRs of both the links are equal.

Fig. 3 presents the outage performance of the considered system for various fading and turbulence parameters; no and significant ($\xi = 1.8$) pointing error; and γ_{th} is set to 10 dB. It is seen that stronger the effect of fading and turbulence, poorer is the outage performance of the system. Moreover, the degradation in the outage performance increases with the unified effect of turbulence and the pointing error. This can be explained by the fact that in case of significant pointing errors, the total impairment of the FSO link is the product of the impairments caused by the turbulence and the pointing errors. For example, at SNR = 40 dB, for $m = 4$, $a = 4$, $b = 4$, $\xi = 2.3$, the outage probability is $P_{out} = 6.308 \times 10^{-4}$ which increases to $P_{out} = 2.08 \times 10^{-2}$ and 1.921×10^{-1} for $m = 2$, $a = 4.2$, $b = 1.4$, $\xi = 2.3$ and $m = 3$, $a = 2$, $b = 0.5$, $\xi = 2.3$, respectively. An interesting observation is made here that the for

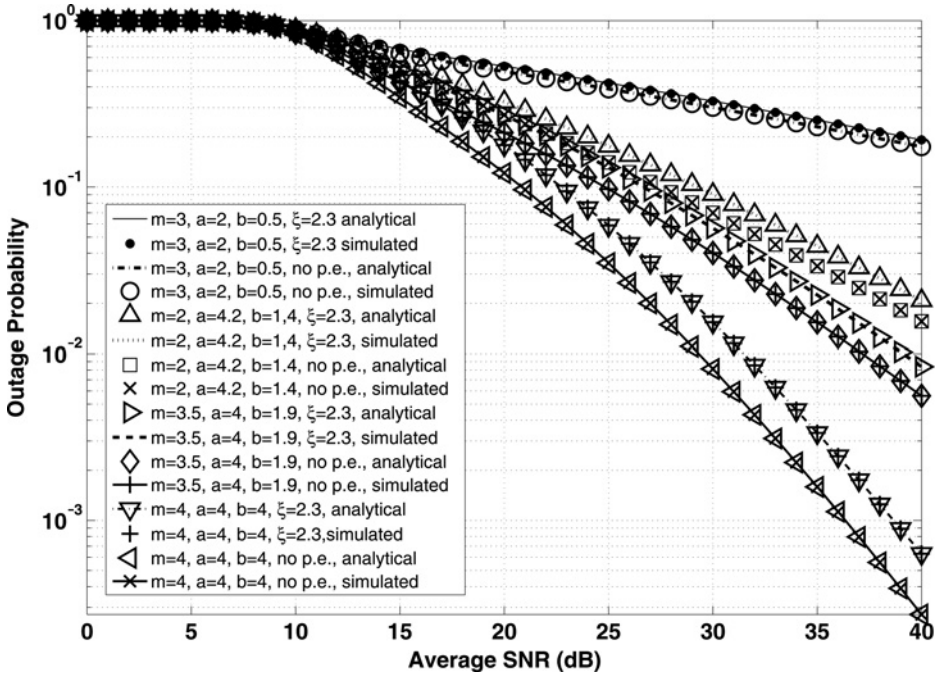

Fig. 3 *Outage probability against average SNR per hop for different values of fading and turbulence parameters, and $\xi = 2.3$*

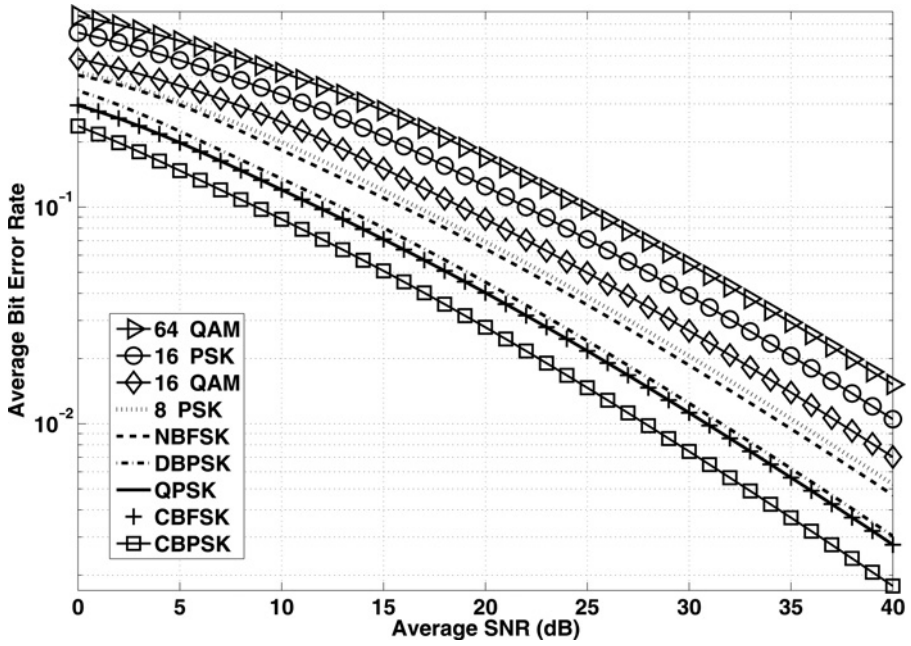

Fig. 4 *Average BER against average SNR per hop for different modulation techniques, when m = 4, a = 4.2, b = 1.4, ξ = 1.3*

moderate turbulence scenario, the effect of pointing error is quite significant. However, under severe turbulence case, the effect of pointing error is negligible as the system is already in highly degraded state.

In Fig. 4, the average BER against the average SNR plots are analysed for various modulation techniques, that is, CBPSK, CBFSK, NBFSK, DBPSK, Q-PSK, 8-PSK, 16-PSK, 16-QAM and 64-QAM with fixed fading statistics and pointing error parameter, $m = 4$, $a = 4.2$, $b = 1.4$ and $\xi = 1.3$. From Fig. 4, it can be observed that CBPSK outperforms the other modulation techniques because it is the most power-efficient modulation technique. Coherent techniques perform better than their corresponding non-coherent techniques because they have the knowledge of the phase of the carrier at the receiver which can be exploited to recover the message signal correctly [27]. Moreover the BER performance is inversely dependent on the minimum Euclidean distance between the symbols in the constellation, that is, as the minimum Euclidean distance between symbols decreases, the BER increases. For example, the minimum Euclidean distance between two constellation points is $0.63E_s$ and $0.39E_s$ for 16-QAM and 16-PSK, respectively. Thus for the same BER, 16-QAM will require 4 dB less SNR than 16-PSK. The *M*-ary techniques are known to be more bandwidth efficient, and the non-coherent schemes does not require phase estimation. Thus the choice of modulation technique depends on the application required and is a trade-off between simplicity, power and bandwidth efficiencies.

Fig. 5 presents the average BER performance of the asymmetric RF-FSO system using CBFSK modulation technique, for different values of fading statistics but fixed pointing error parameter $\xi = 1.2$. It can be seen from the figure that severe the effect of fading and turbulence more is the degradation in the BER performance of the system. For example, at SNR = 40 dB and $\xi = 1.2$, for $m = 3.5$,

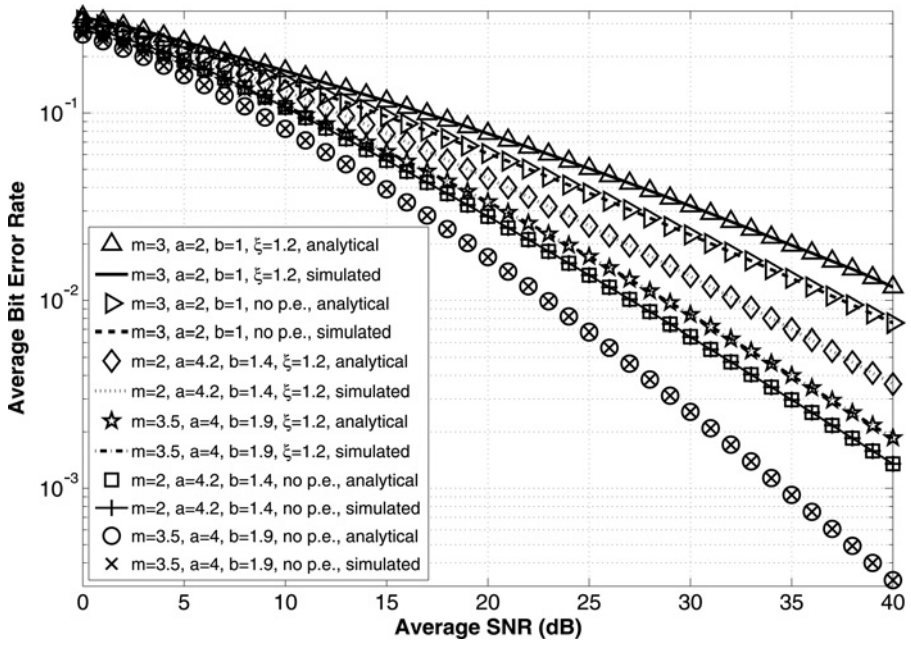

Fig. 5 *Average BER against average SNR per hop for different fading and turbulence conditions in case of CBFSK and ξ = 1.2*

IET Optoelectron., 2015, Vol. 9, Iss. 5, pp. 232–240

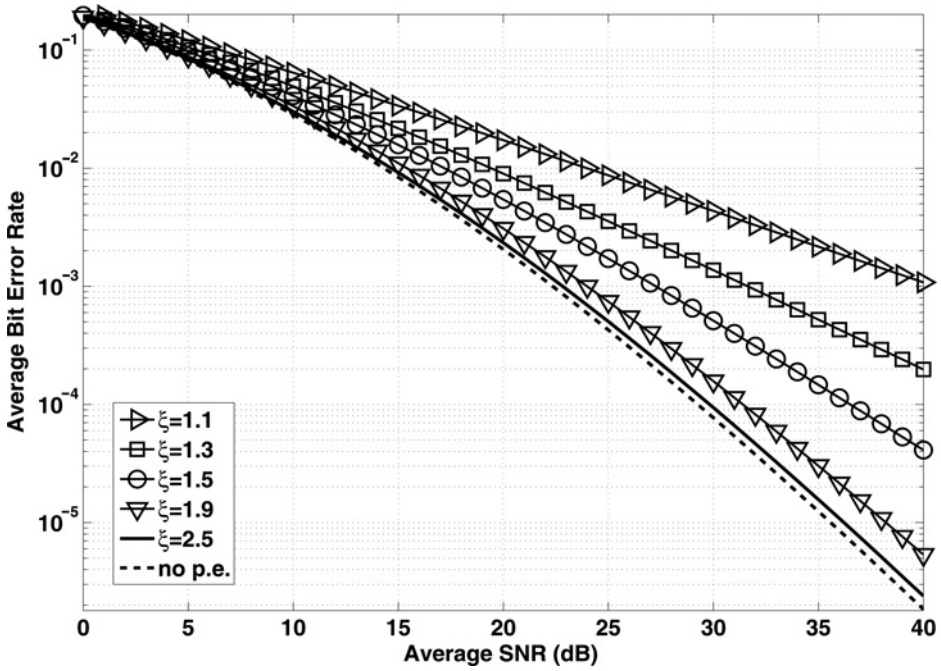

Fig. 6 *Average BER against average SNR per hop for different values of pointing error parameter ξ, in case of CBPSK and m = 4 a = 4 and b = 4*

$a = 4$, $b = 1.9$, the BER is $P_e = 1.856 \times 10^{-3}$ and it increases to $P_e = 3.598 \times 10^{-3}$ and $P_e = 1.177 \times 10^{-2}$, for $m = 2$ $a = 4.2$, $b = 1.4$ and $m = 3$, $a = 2$, $b = 1$, respectively. It can also be seen that the FSO link acts as the dominant link among both of them, as the BER under the strong fading and moderate turbulence is less than the BER under moderate fading and strong turbulence. Similar to Fig. 2. it is observed that the impact of pointing error increases as the severity in the turbulence decreases.

In Fig. 6, the average BER against average SNR plots are analysed under CBPSK and for various values of pointing error parameter, that is, $\xi = 1.1$, 1.3, 1.5, 1.9, 2.5 and no pointing error scenario. The fading parameters are fixed to $m = 4$, $a = 4$, $b = 4$. From the figure, it can be noted that stronger the effect of pointing errors, that is, smaller the value of pointing error parameter ξ, higher is the average BER. This behaviour can be easily understood from the definition of ξ which explains that higher the pointing error displacement standard deviation at the destination, lower is the value of ξ and degraded is the average BER performance of the system. For example, at SNR = 40 dB, the BER, $P_e = 1.84 \times 10^{-6}$, 5.346×10^{-6}, 4.113×10^{-5} and 1.079×10^{-3} for no pointing error scenario, $\xi = 1.9$, 1.5 and 1.1, respectively.

In Fig. 7, we set $\xi = 1.4$ (denoting strong impact of pointing error), to observe the effect of fading and turbulence for various values of m, a and b. It can be observed from Fig. 6, that stronger the effect of atmospheric turbulence, lesser is the capacity of the considered system. For example, at SNR = 20 dB, for $m = 3$, $a = 2$, $b = 4$ and

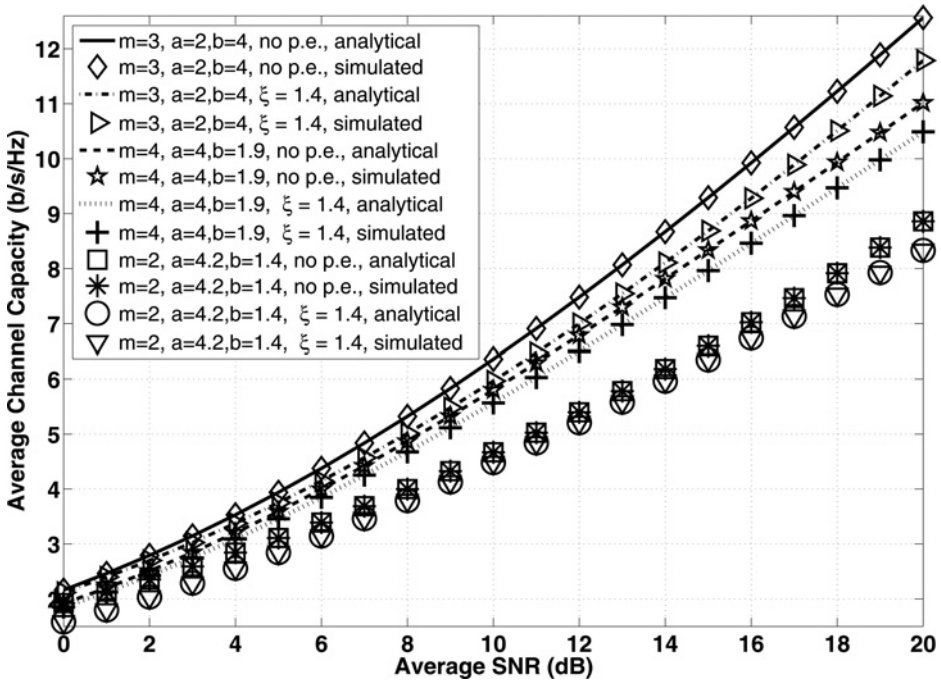

Fig. 7 *Average channel capacity against average SNR per hop for different fading and turbulence conditions with ξ = 1.4*

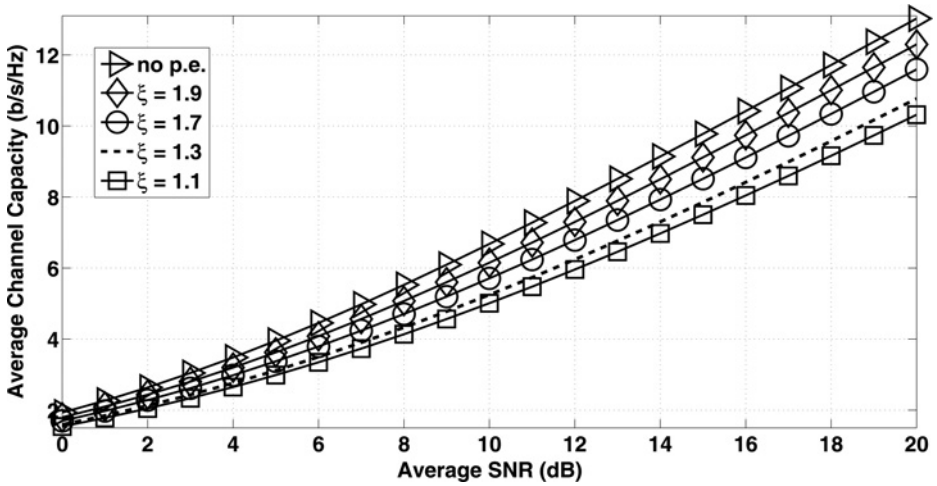

Fig. 8 *Average channel capacity against average SNR per hop for m = 3, a = 4 and b = 4*

$\xi = 1.4$, the capacity degrades approximately by 29.51% when compared with the scenario, where $m = 2$, $a = 4.2$, $b = 1.4$ and $\xi = 1.4$.

In Fig. 8, the capacity against average SNR graph is plotted for varying pointing error parameter, $\xi = 1.2$, 1.7, 2.5 and 3.3; and no pointing errors with fixed moderate turbulence condition, that is, $m = 3$, $a = 4$ and $b = 4$; to study the effect of pointing errors on the capacity of the considered system. It can be observed from Fig. 7 that, under strong effect of pointing error (small values of ξ), the capacity of the considered system is severely degraded. It can be seen from Fig. 7, that in comparison with the scenario for moderate turbulence at both S–R and R–D links, and no pointing error present, the capacity decreases approximately by, 5.77%, 9.62%, 15.38% and 21.15%; for cases when $\xi = 1.9$, 1.7, 1.3, and 1.1, respectively.

It can be observed from Figs. 3, 5 and 7, that the simulation results for the outage probability, the average BER and the channel capacity of the asymmetric RF-FSO system match well with their corresponding analytical results. Moreover it requires only 200 terms in case of turbulence only scenario and 250 terms in case of unified effect scenario, for the analytical results of the capacity of the considered system to match well with the simulated capacity.

6 Conclusions

In this paper, closed-form mathematical expressions have been derived for CDF, PDF and MGF of the equivalent SNR of the DF based dual hop mixed RF-FSO cooperative system. Using these expressions, the novel finite series based analytical expressions for outage probability, the BER and the average capacity of the considered system are obtained. Further the effect of fading, turbulence and pointing error has been investigated on the performance metrics of the Nakagami–Gamma–Gamma asymmetric link. It has been observed that the impact of pointing error is dominant under moderate turbulence scenario, whereas it is negligible in case of very strong turbulence. Moreover in BER plots a clear trend shows that the FSO link acts as the dominant link in the considered dual hop RF-FSO system.

7 References

1 Kedar, D., Aron, S.: 'Urban optical wireless communication networks: The main challenges and possible solutions', *IEEE Commun. Mag.*, 2004, **42**, (5), pp. S2–S7
2 Andrews, L., Phillips, R., Hopen, C.: 'Laser beam scintillation with applications' (SPIE Press, New York, USA, 2001)
3 Bekkali, A., Naila, C.B., Kazaura, K., *et al.*: 'Transmission analysis of OFDM-based wireless services over turbulent Radio-on-FSO links modeled by Gamma–Gamma distribution', *IEEE Photonics J.*, 2010, **2**, (3), pp. 510–520
4 Moradi, H., Falahpour, M., Refai, H., *et al.*: 'On the Capacity of hybrid FSO/RF links'. Proc. IEEE GLOBECOM, Miami, FL, December 2010, pp. 1–5
5 Tsiftsis, T.A., Sandalidis, H.G., Karagiannidis, G.K., *et al.*: 'Optical wireless links with spatial diversity over strong atmospheric turbulence channels', *IEEE Trans. Wirel. Commun.*, 2009, **8**, (2), pp. 951–957
6 Safari, M., Uysal, M.: 'Relay-assisted free-space optical communication', *IEEE Trans. Wirel. Commun.*, 2008, **7**, (12), pp. 5441–5449
7 Lee, E., Park, J., Han, D., *et al.*: 'Performance analysis of the asymmetric dual-hop relay transmission with mixed RF/FSO links', *IEEE Photon. Technol. Lett.*, 2011, **23**, (1), pp. 1642–1644
8 Bhatnagar, M.R.: 'Performance analysis of decode-and-forward relaying in Gamma-Gamma fading channels', *IEEE Photon. Technol. Lett.*, 2012, **24**, (7), pp. 545–547
9 Bhatnagar, M.R.: 'Average BER analysis of differential modulation in DF cooperative communication system over Gamma-Gamma fading FSO links', *IEEE Commun. Lett.*, 2012, **16**, (8), pp. 1228–1231
10 Anees, S., Bhatnagar, M.R.: 'On the capacity of decode-and-forward dual-hop free space optical communication systems'. Proc. IEEE Wireless Communication and Network Conf. (WCNC), 6–9 April 2014, pp. 18–23
11 Anees, S., Bhatnagar, M.R.: 'Performance of an amplify-and-forward dual-hop asymmetric RF-FSO communication system', *J. Opt. Commun. Netw.*, 2015, **7**, (2), pp. 124–135
12 Nistazakis, H.E., Karagianni, E.A., Tsigopoulos, A.D., *et al.*: 'Average capacity of optical wireless communication systems over atmospheric turbulence channels', *J. Lightw. Technol.*, 2009, **27**, (8), pp. 974–979
13 Popoola, W.O., Ghassemlooy, Z.: 'BPSK subcarrier intensity modulated free-space optical communications in atmospheric turbulence', *IEEE/OSA J. Lightw. Technol.*, 2009, **27**, (8), pp. 967–973
14 Samimi, H., Uysal, M.: 'End-to-End performance of mixed RF/FSO transmission systems', *J. Opt. Commun. Netw.*, 2013, **5**, (11), pp. 1139–1144
15 Peppas, K.P., Stassinakis, A.N., Nistazakis, H.E., *et al.*: 'Capacity analysis of dual amplify-and-forward relayed free-space optical communication systems over turbulence channels with pointing errors', *IEEE J. Opt. Commun. Netw.*, 2013, **5**, (9), pp. 1032–1042
16 Miridakis, N.I., Matthaiou, M., Karagiannidis, G.K.: 'Multiuser relaying over mixed RF/FSO links', *IEEE Trans. Commun.*, 2014, **62**, (5), pp. 1634–1645
17 Laneman, J.N., Tse, D.N.C., Wornell, G.W.: 'Cooperative diversity in wireless networks: Efficient protocols and outage behavior', *IEEE Trans. Inf. Theory*, 2004, **50**, (11), pp. 3062–3080
18 Niu, M., Cheng, J., Holzman, J.F.: 'Error rate performance comparison of coherent and subcarrier intensity modulated optical wireless communications', *J. Opt. Commun. Netw.*, 2013, **5**, (6), pp. 554–564
19 Prudnikov, A.P., Brychkov, Y.A., Marichev, O.I.: 'Integrals and Series' (Gordon and Breach Science Publishers, New York, USA, 1990)
20 Tang, X., Wang, Z., Xu, Z., *et al.*: 'Multihop free-space optical communications over turbulence channels with pointing errors using heterodyne detection', *J. Lightw. Technol.*, 2014, **32**, (15), pp. 2597–2604
21 Papoulis, A., Pillai, S.U.: 'Probability, Random variables and stochastic Processes' (Tata Mcgraw-Hill, 2002, 4th edn.)
22 Luke, Y.L.: 'The special functions and their approximation' (Academic Press, New York, 1969, 1st edn.)
23 Ansari, I.S., Ahmadi, S.A., Yilmaz, F., *et al.*: 'A new formula for the BER of binary modulations with dual-branch selection over generalized-K composite fading channels', *IEEE Trans. Commun.*, 2011, **59**, (10), pp. 2654–2658
24 Bhatnagar, M.R., Arti, M.K.: 'On the closed-form performance analysis of maximal ratio combining in Shadowed-Rician fading LMS channels', *IEEE Commun. Lett.*, 2014, **18**, (1), pp. 54–57
25 Yilmaz, F., Alouini, M.-S.: 'A unified MGF-based capacity analysis of diversity combiners over generalized fading channels', *IEEE Trans. Commun.*, 2012, **60**, (3), pp. 862–875
26 Ijaz, M., Ghassemlooy, Z., Pesek, J., *et al.*: 'Modeling of fog and smoke attenuation in free space optical communications link under controlled laboratory conditions', *IEEE/OSA J. Lightw. Technol.*, 2013, **31**, (11), pp. 1720–1726
27 Proakis, J.G., Salehi, M.: 'Digital communications' (Mc Graw Hill Higher Educations, 2007, 5th edn.)